

TornadoAggregate: Accurate and Scalable Federated Learning via the Ring-Based Architecture

Jin-woo Lee,¹ Jaehoon Oh,¹ Sungsu Lim,² Se-Young Yun,¹ Jae-Gil Lee,¹

¹ Korea Advanced Institute of Science and Technology

² Chungnam National University

jinwoo.lee@kaist.ac.kr, jhoon.oh@kaist.ac.kr, sungsu@cnu.ac.kr, yunseyoung@kaist.ac.kr, jaegil@kaist.ac.kr

Abstract

Federated learning has emerged as a new paradigm of collaborative machine learning; however, many prior studies have used global aggregation along a star topology without much consideration of the communication scalability or the diurnal property relied on clients' local time variety. In contrast, ring architecture can resolve the scalability issue and even satisfy the diurnal property by iterating nodes without an aggregation. Nevertheless, such ring-based algorithms can inherently suffer from the high-variance problem. To this end, we propose a novel algorithm called *TornadoAggregate* that improves both accuracy and scalability by facilitating the ring architecture. In particular, to improve the accuracy, we reformulate the loss minimization into a variance reduction problem and establish three principles to reduce variance: Ring-Aware Grouping, Small Ring, and Ring Chaining. Experimental results show that TornadoAggregate improved the test accuracy by up to 26.7% and achieved near-linear scalability.

1 Introduction

Federated learning (Konečný et al. 2016a; McMahan et al. 2017b) enables mobile devices to collaboratively learn a shared model while keeping all training data on the devices, thus avoiding data transfer to the cloud or central server. One of the main reasons for this recent boom in federated learning is that it does not compromise user privacy. In this framework, star architecture (Figure 1(a)), which involves a central parameter server aggregating and broadcasting locally learned models, has been most widely adopted in favor of its simple distributed parallelism. However, the star architecture can easily become a communication bottleneck and cannot take into account the diurnal property of federated learning (McMahan et al. 2017a; Eichner et al. 2019), in which the global data distribution of clients significantly varies due to the difference in the clients' local time.

Ring architecture (Figure 1(b)), in contrast, can resolve the scalability issue and even satisfy the diurnal property by iterating nodes without a central coordinator. In addition, it has the potential to improve accuracy through an unbiased estimation of conventional centralized learning at the expense of communication cost. Notably, Duan et al. (2020) proposed a star architecture with ring-based groups,

Copyright © 2021, Association for the Advancement of Artificial Intelligence (www.aaai.org). All rights reserved.

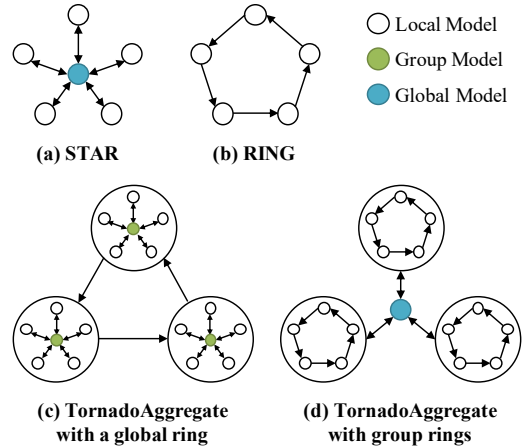


Figure 1: Representative architectures and proposed ring-based algorithm TornadoAggregate.

while Ding et al. (2020) proposed a ring architecture with stars-based groups. Ghosh et al. (2020) and Eichner et al. (2019) proposed star-based and ring-based groups, respectively, without global communication. Other than the importance of addressing the problem, less has been addressed how a ring-based architecture should be developed from the perspective of both accuracy and scalability.

In this paper, we propose a novel *TornadoAggregate* algorithm that improves both accuracy and scalability by facilitating the ring architecture. To improve accuracy, in particular, TornadoAggregate aims at reducing the variance inherent in a ring iteration by considering three principles: *ring-aware grouping*, *small ring*, and *ring chaining*. Based on the *ring-aware grouping* principle, for the TornadoAggregate with a global ring (Figure 1(c)) and group rings (Figure 1(d)), nodes are grouped such that it reduces the inter-group variance in the global ring and inter-node variance in each group ring, respectively; the number of groups is adjusted to satisfy the *small ring* principle, thus achieving the small variance; we introduce *ring chaining* technique to increase the batch size with high node utilization in a ring, leading to the reduced variance.

We confirmed that TornadoAggregate achieved a higher accuracy by up to 26.7% and near-linear scalability.

Architecture	Convergence Bound	Communication Scalability
<i>STAR</i>	$O(Dh(\tau))$	$O(\mathcal{N})$
<i>RING</i>	0 (Approximate)	$O(1)$
<i>STAR-stars</i>	$O(\Delta h(\tau_1\tau_2) + \delta h(\tau_1))$	$O(\mathcal{N})$
<i>STAR-rings</i>	$O(Dh(\tau_1\tau_2))$ (Approximate)	$O(\mathcal{G})$
<i>RING-stars</i>	$O(Dh(\tau_1))$ (Approximate)	$O(\mathcal{N} / \mathcal{G})$
<i>RING-rings</i>	0 (Approximate)	$O(1)$
<i>stars</i>	$O(\delta h(\tau))$	$O(\mathcal{N})$
<i>rings</i>	0 (Approximate)	$O(\mathcal{G})$

Table 1: **Comparison of architectures.** $|\mathcal{N}|$ and $|\mathcal{G}|$ denote the number of nodes and groups, respectively. D , δ , and Δ denote the local-to-global, local-to-group, and group-to-global divergence, respectively.

2 Architectures of Federated Learning

We first briefly describe *federated learning* and then survey relevant architectures in terms of *accuracy* and *scalability*.

Basics of Federated Learning

The objective of *federated learning* is to find an approximate solution of Eq. (1) (McMahan et al. 2017b). Here, $F(\mathbf{w})$ is the loss of predictions with a model \mathbf{w} over the set of all data examples $\mathcal{D} \triangleq \cup_{i \in \mathcal{N}} \mathcal{D}^i$ across all nodes, where \mathcal{N} is the set of node indices, and $F^i(\mathbf{w}) \triangleq \sum_{(\mathbf{x}, y) \in \mathcal{D}^i} \frac{1}{|\mathcal{D}^i|} l(\mathbf{w}, \mathbf{x}, y)$ is the loss of predictions with a loss function l parameterized by \mathbf{w} over the set of data examples $(\mathbf{x}, y) \in \mathcal{D}^i$ on node i .

$$\min_{\mathbf{w} \in \mathbb{R}^d} F(\mathbf{w}) \text{ where } F(\mathbf{w}) \triangleq \sum_{i \in \mathcal{N}} \frac{|\mathcal{D}^i|}{|\mathcal{D}|} F^i(\mathbf{w}) \quad (1)$$

To resolve Eq. (1), a huge number of architectures are being actively proposed, and based on hierarchical composition, they can be classified into *three* main categories: *flat*, *consensus group*, and *pluralistic group*. Table 1 compares them in terms of convergence bound and scalability, each of which is analyzed in Appendix A and B, respectively.

Flat Architecture

Flat represents an architecture without hierarchical composition that, in turn, includes *STAR* and *RING* architecture. *STAR* is the same as the canonical FedAvg (McMahan et al. 2017b) without node sampling, as defined by Definition 1.

Definition 1. *STAR* involves local update, which learns each local model \mathbf{w}^i with learning rate η by performing gradient descent steps, and *global aggregation*, which learns the global model \mathbf{w} by aggregating all \mathbf{w}^i along a star topology and synchronizes \mathbf{w}^i with \mathbf{w} every τ epochs, as in Eq. (2).

$$\mathbf{w}_t^i \triangleq \begin{cases} \mathbf{w}_{t-1}^i - \eta \nabla F^i(\mathbf{w}_{t-1}^i) & \text{if } t \bmod \tau \neq 0 \\ \mathbf{w}_t & \text{if } t \bmod \tau = 0 \end{cases} \quad (2)$$

where $\mathbf{w}_t \triangleq \sum_{i \in \mathcal{N}} \frac{|\mathcal{D}^i|}{|\mathcal{D}|} [\mathbf{w}_{t-1}^i - \eta \nabla F^i(\mathbf{w}_{t-1}^i)]$

STAR exhibits the most simple distributed parallelism that, at the same time, leads to low scalability of $O(|\mathcal{N}|)$ due to the communication bottleneck in global aggregation.

In contrast, *RING* (Li et al. 2018; Eichner et al. 2019) resolves the aforementioned scalability issue by removing the global aggregation, as defined by Definition 2.

Definition 2. *RING* extends *STAR* by replacing the global aggregation with *global inter-node transfer* that synchronizes a new model \mathbf{w}^{i_j} on node i_j with the previously learned model $\mathbf{w}^{i_{j-1}}$ on node i_{j-1} every τ epoch along a certain ring topology¹ $[i_j \in \mathcal{N} | j = \lfloor t/\tau \rfloor, i_{j+|\mathcal{N}|} = i_j]$ with a period $|\mathcal{N}|$ to satisfy the diurnal property, as in Eq. (3).

$$\mathbf{w}_t^{i_j} \triangleq \begin{cases} \mathbf{w}_{t-1}^{i_j} - \eta \nabla F^{i_j}(\mathbf{w}_{t-1}^{i_j}) & \text{if } t \bmod \tau \neq 0 \\ \mathbf{w}_t^{i_{j-1}} & \text{if } t \bmod \tau = 0 \end{cases} \quad (3)$$

RING exhibits low convergence bound, attributed to Theorem 1, and benefits from high scalability of $O(1)$. However, it is considered impractical in federated learning, where a large $|\mathcal{N}|$ is assumed, because it takes $|\mathcal{N}|$ times as much communication rounds to iterate a global epoch as *STAR*.

Theorem 1. *RING* is an unbiased estimator of the centralized learning that learns a centralized model by assuming the federated datasets to be located at centralized storage.

Owing to lack of space, we defer all proofs to Appendix C.

Consensus Group Architecture

Consensus group represents an architecture with group hierarchy and global communication to reach a global consensus among groups, which, in turn, includes *four* architectural combinations: *STAR-stars*, *STAR-rings*, *RING-stars*, and *RING-rings*. First, *STAR-stars* (Lin et al. 2018; Bonawitz et al. 2019; Liu et al. 2020; Luo et al. 2020; Abad et al. 2020) mitigates the non-IID issue via group-based learning (Zhao et al. 2018), which leads to improved accuracy, as defined by Definition 3.

Definition 3. *STAR-stars* extends *STAR* by additionally allowing multiple intermediate group star aggregations, thus postfixed by *stars*. In particular, the set of all node indices \mathcal{N} is partitioned into sets of node indices for $|\mathcal{G}|$ node groups $\{\mathcal{N}^k\}_{k=1 \dots |\mathcal{G}|}$, where $\cup_{k \in \mathcal{G}} \mathcal{N}^k = \mathcal{N}$ and $\forall k \neq l, \mathcal{N}^k \cap \mathcal{N}^l = \emptyset$, and $\mathcal{D}^k \triangleq \cup_{i \in \mathcal{N}^k} \mathcal{D}^{k,i}$. Then, for each group, it learns the group model \mathbf{w}^k by aggregating all local models $\mathbf{w}^{k,i}$ along a group star topology and synchronizes $\mathbf{w}^{k,i}$ with \mathbf{w}^k every τ_1 epochs, as shown by Eq. (4). Similar to Eq. (2), a global aggregation is performed every $\tau_1\tau_2$ steps.

$$\mathbf{w}_t^{k,i} \triangleq \begin{cases} \mathbf{w}_{t-1}^{k,i} - \eta \nabla F^{k,i}(\mathbf{w}_{t-1}^{k,i}) & \text{if } t \bmod \tau_1 \neq 0 \\ \mathbf{w}_t^k & \text{if } t \bmod \tau_1 = 0, \\ & t \bmod \tau_1\tau_2 \neq 0 \\ \mathbf{w}_t & \text{if } t \bmod \tau_1\tau_2 = 0 \end{cases} \quad (4)$$

where $\mathbf{w}_t^k \triangleq \sum_{i \in \mathcal{N}^k} \frac{|\mathcal{D}^{k,i}|}{|\mathcal{D}^k|} [\mathbf{w}_{t-1}^{k,i} - \eta \nabla F^{k,i}(\mathbf{w}_{t-1}^{k,i})]$

and $\mathbf{w}_t \triangleq \sum_{k \in \mathcal{G}} \frac{|\mathcal{D}^k|}{|\mathcal{D}|} \mathbf{w}_t^k$

¹As long as the conditions are satisfied, a ring can be defined in any way (e.g., a random permutation in Algorithm 1).

STAR-stars is known to improve *STAR* under certain parameter settings in favor of the non-IID mitigation (Liu et al. 2020), but it exhibits the low scalability of $O(|\mathcal{N}|)$.

Next, analogous to the development of *RING*, *STAR-rings* (Duan et al. 2020), *RING-stars* (So, Guler, and Avestimehr 2020; Ding et al. 2020), and *RING-rings* (Eichner et al. 2019) also aim at improving both convergence bound and scalability while sacrificing communication cost, which are summarized in Table 1. Formal definitions are as follows.

Definition 4. Similar to Definition 2, *STAR-rings* extends *STAR-stars* by replacing the group aggregation with *group inter-node transfer* that, for each group $k \in \mathcal{G}$, synchronizes a new model \mathbf{w}^{k,i_j} on node $i_j \in \mathcal{N}^k$ with the previously learned model $\mathbf{w}^{k,i_{j-1}}$ on node i_{j-1} every τ_1 epochs along a certain ring topology $[i_j \in \mathcal{N}^k | j = \lfloor t/\tau_1 \rfloor, i_{j+|\mathcal{N}^k|} = i_j]$ with a period $|\mathcal{N}^k|$ to satisfy the diurnal property within each group. In short, $\mathbf{w}_t^{k,i} \triangleq \mathbf{w}_t^k$ (group aggregation) of Eq. (4) is replaced with $\mathbf{w}_t^{k,i_j} \triangleq \mathbf{w}_t^{k,i_{j-1}}$ (group inter-node transfer).

Definition 5. Similar to Definition 4, *RING-stars* extends *STAR-stars* by replacing the global aggregation with *global inter-group transfer* that synchronizes a new local model $\mathbf{w}^{k_l,i}$ on node $i \in \mathcal{N}^{k_l}$ with the previously learned group model \mathbf{w}^{k_l-1} in group k_{l-1} every $\tau_1\tau_2$ steps along a certain ring topology $[k_l \in \mathcal{G} | l = \lfloor t/(\tau_1\tau_2) \rfloor, k_{l+|\mathcal{G}|} = k_l]$ with a period $|\mathcal{G}|$ to satisfy the diurnal property across all groups. In short, $\mathbf{w}_t^{k,i} \triangleq \mathbf{w}_t^k$ (global aggregation) of Eq. (4) is replaced with $\mathbf{w}_t^{k_l,i} \triangleq \mathbf{w}_t^{k_{l-1}}$ (global inter-group transfer).

Definition 6. *RING-rings* extends *STAR-stars* by replacing the group and global aggregation with the group inter-node and global inter-group transfer, respectively.

Similar to *RING*, *RING-rings* is considered impractical in federated learning due to large number of nodes.

Pluralistic Group Architecture

Pluralistic group represents an architecture with group hierarchy and without global communication to develop more independent and specialized group models than the aforementioned consensus model, which leads to decreased non-IIDness, and consequently, improved accuracy. Representative *pluralistic group* includes *stars* and *rings*. Recently, *stars* (Ghosh et al. 2019, 2020; Xie et al. 2020; Briggs et al. 2020; Sattler, Müller, and Samek 2020) has received great attention, which is defined by Definition 7.

Definition 7. *stars* is defined as *STAR-stars* without global aggregation. Unlike Eq. (4), $\mathbf{w}_t^{k,i}$ is not synchronized with \mathbf{w}_t and thus group communication rounds τ_2 is not defined.

Definition 8. Similar to Definition 7, *rings* is defined as *STAR-rings* without global aggregation.

It is important to note that the growing popularity of pluralistic group architectures may be hype. According to Theorem 2, *stars* may achieve lower accuracy than *STAR*.

Theorem 2. The convergence bound $O(\delta h(\tau))$ of *stars* doesn't necessarily be better than $O(Dh(\tau))$ of *STAR*.

Lastly, as shown in Table 1, *rings* can benefit from the low convergence bound as well as high scalability of $O(|\mathcal{G}|)$.

3 Reformulation: Variance Reduction

As previously noted, ring-based architectures such as *RING*, *STAR-rings*, *RING-stars*, *Ring-rings*, and *rings* have great potential to improve both accuracy and scalability. However, the convergence analysis framework introduced in this study is mostly based on unbiasedness property to easily compare all of the architectures. To better understand architectures from the perspective of accuracy, the variance should also be further considered. To this end, based on Theorem 3, we reformulate the problem of Eq. (1) to the variance reduction of ring-based architectures.

Theorem 3. *RING* exhibits higher variance than the centralized learning (unbiased estimator of *RING* from Theorem 1).

4 Proposed Algorithm: TornadoAggregate

The ring-based federated learning under high variance issue looks similar to the continual learning under catastrophic forgetting (Parisi et al. 2019), but the former additionally involves partitioned data groups as well as data iteration along a ring. Considering the differences, we establish *three* principles to reduce variance.

- **Principle 1 (Ring-Aware Grouping):** For architectures with group rings, nodes should be clustered so that inter-node variance becomes low within a group. On the other hand, for architectures with a global ring, nodes should be IID grouped so that inter-group variance becomes low.
- **Principle 2 (Small Ring):** It is straightforward that, the smaller a ring, the lower its iteration variance.
- **Principle 3 (Ring Chaining):** A ring can have multiple iteration chains (Ding et al. 2020), each of which iterates the same ring at a different starting node and thus learns an unbiased model different from each other. Multiple chains can reduce learning variance, which is attributed to the reduced variance from increased batch size.

Based on the abovementioned principles, we propose a novel ring-based algorithm called *TornadoAggregate* and derive *two* heuristics according to the architecture type. We refer to *TornadoAggregate* with *RING-stars* and *STAR-rings* as *Tornado* and *Tornadoes*, respectively. In particular, for the *ring-aware grouping* principle, *Tornado* and *Tornadoes* require nodes to be IID grouped and clustered, respectively; for the *small ring* principle, *Tornado* and *Tornadoes* require a small and large number of groups, respectively; for the *ring chaining* principle, both require a large number of chains.

As shown in Algorithm 1, *Tornado* takes the node set \mathcal{N} and the number of groups $|\mathcal{G}|$, chains C , epochs τ_1 , and communication rounds τ_2 as input and returns the final model \mathbf{w}_T as output. It begins by initializing all local models $\mathbf{w}_0^{k,i}$, a randomly permuted inter-group ring $[k_l]$, and group indices $\{\mathcal{N}^{k_l}\}$ via the IID node grouping (Lines 1–3). Then, for each chain and each node, the local updates are performed (Lines 5–8); each group model is learned by aggregating all local models every τ_1 epochs (Lines 9–10) and is transferred to all nodes in the next group k_{next} every $\tau_1\tau_2$ steps (Lines 11–13). Overall, Lines 4–13 repeat for T steps.

Because *Tornado* and *Tornadoes* are inherently correlated, we defer the description of *Tornadoes* to Appendix D.

Algorithm 1: Tornado (RING-stars)

INPUT : $\mathcal{N}, |\mathcal{G}|, C, \tau_1, \tau_2$
OUTPUT: \mathbf{w}_T

- 1 Initialize $\{\mathbf{w}_0^{k,i}\}_{i \in \mathcal{N}}$ to a random model \mathbf{w}_0
- 2 Initialize a random ring $[k_l \in \mathcal{G} | l \in \mathbb{N}^0, k_{l+|\mathcal{G}|} = k_l]$
- 3 $\{\mathcal{N}^k\}_{k \in \mathcal{G}} \leftarrow \text{GROUP_BY_IID}(\mathcal{N})$ // Algorithm 3
- 4 **for** $t \leftarrow 0, \dots, T - 1$ **do**
- 5 **for each** chain $c \leftarrow 0, \dots, C - 1$ **in parallel do**
- 6 $l \leftarrow \lfloor t / (\tau_1 \tau_2) \rfloor, k \leftarrow (k_l + c) \bmod |\mathcal{G}|$
- 7 **for each** node $i \in \mathcal{N}^k$ **in parallel do**
- 8 $\mathbf{w}_{t+1}^{k,i} \leftarrow \mathbf{w}_t^{k,i} - \eta \nabla F^{k,i}(\mathbf{w}_t^{k,i})$
- 9 **if** $t \bmod \tau_1$ **and** $t \bmod \tau_1 \tau_2 \neq 0$ **then**
- 10 $\{\mathbf{w}_t^{k,i}\}_{i \in \mathcal{N}^k} \leftarrow \sum_{i \in \mathcal{N}^k} \frac{|\mathcal{D}^{k,i}|}{|\mathcal{D}^k|} \mathbf{w}_t^{k,i}$
- 11 **if** $t \bmod \tau_1 \tau_2 = 0$ **then**
- 12 $k_{next} \leftarrow (k_{l+1} + c) \bmod |\mathcal{G}|$
- 13 $\{\mathbf{w}_t^{k_{next},i}\}_{i \in \mathcal{N}^{k_{next}}} \leftarrow \sum_{i \in \mathcal{N}^k} \frac{|\mathcal{D}^{k,i}|}{|\mathcal{D}^k|} \mathbf{w}_t^{k,i}$

Algorithm	Architecture	Group Type	# Chain
FedAvg(McMahan et al.)	<i>STAR</i>	-	-
IFCA(Ghosh et al.)	<i>stars</i>	Cluster	-
HierFAVG(Liu et al.)	<i>STAR-stars</i>	Random	-
Astraea(Duan et al.)	<i>STAR-rings</i>	IID	1
MM-PSGD(Ding et al.)	<i>RING-stars</i>	Cluster	1
Tornado (Proposed)	<i>RING-stars</i>	IID	$ \mathcal{G} $
Tornadoes (Proposed)	<i>STAR-rings</i>	Cluster	$ \mathcal{G} $

Table 2: Comparison of algorithms.

5 Evaluation

Experimental Setting

Benchmark Datasets and Models We used *two* official benchmark datasets and models provided by FedML.

- **FedShakespeare on RNN** consists of 715 nodes with 16068 train and 2356 test examples. RNN is the same as the one proposed by McMahan et al. (2017b).
- **MNIST on logistic regression** consists of 1000 nodes with 10 classes of 61664 train and 7371 test examples.

Algorithms In Table 2, the proposed Tornado and Tornadoes are compared with *five* state-of-the-art algorithms in terms of group type and number of chains. Used parameters are summarized in Appendix E. We evaluate each algorithm five times and report the average with standard deviation.

Results

Figure 2 shows the test accuracy for FedShakespeare dataset. Tornadoes outperformed the state-of-the-art algorithms by up to 26.7% and the next best group (Tornado, FedAvg, and HierFAVG) by 4.4% on average. The low performance of Tornado relative to Tornadoes is attributed to the communication interval; Tornado(*RING-stars*) takes $\tau_1 \tau_2$ steps for a global inter-group transfer in the *RING*, which is larger than τ_1 steps of Tornadoes(*STAR-rings*) for a group inter-node transfer in each *ring*, thus causing higher divergence. The

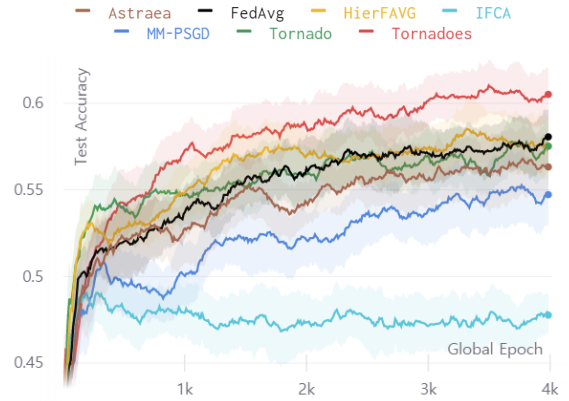


Figure 2: Test accuracy for FedShakespeare.

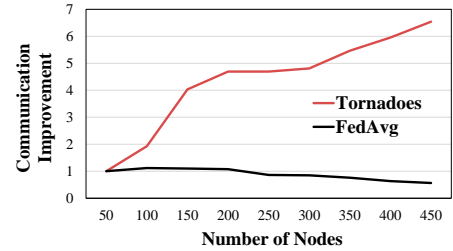


Figure 3: Communication scalability to node size.

poor performances of Astraea and MM-PSGD come from the high variance caused by the inappropriate node grouping and low chain utilization. Lastly, IFCA achieved the worst accuracy due to the difficulty of clustering FedShakespeare dataset, as explained by the small clustering cost reduction of only 4.3%, in which case the relationship between FedAvg and IFCA is consistent with Theorem 2.

Figure 3 shows the communication scalability to the number of nodes ranging from 50 to 500 for MNIST dataset. For each case, we measured the communication data size in bytes to reach the converged train accuracy of the case with 50 nodes (73% for FedAvg and 79% for Tornadoes) and showed the improvement relative to that case. Tornadoes achieved near-linear scalability, which is attributed to the superior communication scalability cost of *STAR-rings*.

6 Conclusion

In this paper, we provided a comprehensive survey of learning architectures in terms of accuracy and scalability. Our formal analysis led to the necessity of ring-based architecture and its inherent variance reduction problem. To this end, we proposed a novel ring-based algorithm **TornadoAggregate** that improves both scalability and accuracy by reducing variance in a ring iteration. Experimental results show that, compared with the state-of-the-art algorithms, TornadoAggregate improved the test accuracy by up to 26.7% and achieved near-linear scalability. Overall, we believe that our novel ring-based algorithm has made important steps towards accurate and scalable federated learning.

References

- Abad, M. S. H.; Ozfatura, E.; Gunduz, D.; and Ercetin, O. 2020. Hierarchical federated learning across heterogeneous cellular networks. In *ICASSP 2020-2020 IEEE Int'l. Conf. Acoustics, Speech and Signal Processing (ICASSP)*, 8866–8870. IEEE.
- Bonawitz, K.; Eichner, H.; Grieskamp, W.; Huba, D.; Ingerman, A.; Ivanov, V.; Kiddon, C.; Konečný, J.; Mazzocchi, S.; McMahan, H. B.; et al. 2019. Towards federated learning at scale: System design. *arXiv:1902.01046*.
- Briggs, C.; Fan, Z.; Andras, P.; and Andras, P. 2020. Federated learning with hierarchical clustering of local updates to improve training on non-IID data. *arXiv:2004.11791*.
- Caldas, S.; Konečný, J.; McMahan, H. B.; and Talwalkar, A. 2018. Expanding the reach of federated learning by reducing client resource requirements. *arXiv:1812.07210*.
- Ding, Y.; Niu, C.; Yan, Y.; Zheng, Z.; Wu, F.; Chen, G.; Tang, S.; and Jia, R. 2020. Distributed Optimization over Block-Cyclic Data. *arXiv:2002.07454*.
- Duan, M.; Liu, D.; Chen, X.; Liu, R.; Tan, Y.; and Liang, L. 2020. Self-balancing federated learning with global imbalanced data in mobile systems. *IEEE Transactions on Parallel and Distributed Systems* 32(1): 59–71.
- Eichner, H.; Koren, T.; McMahan, H. B.; Srebro, N.; and Talwar, K. 2019. Semi-cyclic stochastic gradient descent. *arXiv:1904.10120*.
- Ghosh, A.; Chung, J.; Yin, D.; and Ramchandran, K. 2020. An Efficient Framework for Clustered Federated Learning. *arXiv:2006.04088*.
- Ghosh, A.; Hong, J.; Yin, D.; and Ramchandran, K. 2019. Robust federated learning in a heterogeneous environment. *arXiv:1906.06629*.
- He, C.; Avestimehr, S.; and Annavaram, M. 2020. Group knowledge transfer: Collaborative training of large cnns on the edge. *arXiv:2007.14513*.
- He, C.; Li, S.; So, J.; Zhang, M.; Wang, H.; Wang, X.; Vepakomma, P.; Singh, A.; Qiu, H.; Shen, L.; Zhao, P.; Kang, Y.; Liu, Y.; Raskar, R.; Yang, Q.; Annavaram, M.; and Avestimehr, S. 2020. FedML: A Research Library and Benchmark for Federated Machine Learning. *arXiv:2007.13518*.
- Hegedűs, I.; Danner, G.; and Jelasity, M. 2019. Gossip learning as a decentralized alternative to federated learning. In *IFIP Int'l Conf. Distributed Applications and Interoperable Systems*, 74–90. Springer.
- Jeong, E.; Oh, S.; Kim, H.; Park, J.; Bennis, M.; and Kim, S.-L. 2018. Communication-efficient on-device machine learning: Federated distillation and augmentation under non-iid private data. *arXiv:1811.11479*.
- Konečný, J.; McMahan, H. B.; Ramage, D.; and Richtárik, P. 2016a. Federated optimization: Distributed machine learning for on-device intelligence. *arXiv:1610.02527*.
- Konečný, J.; McMahan, H. B.; Yu, F. X.; Richtárik, P.; Suresh, A. T.; and Bacon, D. 2016b. Federated learning: Strategies for improving communication efficiency. In *NIPS 2016 Workshop on Private Multi-Party Machine Learning*.
- Li, D.; and Wang, J. 2019. Fedmd: Heterogenous federated learning via model distillation. *arXiv:1910.03581*.
- Li, X.; Huang, K.; Yang, W.; Wang, S.; and Zhang, Z. 2020. On the convergence of fedavg on non-iid data. In *Int'l Conf. Learning Representations*.
- Li, Y.; Yu, M.; Li, S.; Avestimehr, S.; Kim, N. S.; and Schwing, A. 2018. Pipe-sgd: A decentralized pipelined sgd framework for distributed deep net training. In *Advances in Neural Information Processing Systems*, 8045–8056.
- Lin, T.; Stich, S. U.; Patel, K. K.; and Jaggi, M. 2018. Don't Use Large Mini-Batches, Use Local SGD. *arXiv:1808.07217*.
- Liu, L.; Zhang, J.; Song, S.; and Letaief, K. B. 2020. Client-edge-cloud hierarchical federated learning. In *ICC 2020-2020 IEEE Int'l. Conf. Communications (ICC)*, 1–6. IEEE.
- Luo, S.; Chen, X.; Wu, Q.; Zhou, Z.; and Yu, S. 2020. HFEL: Joint Edge Association and Resource Allocation for Cost-Efficient Hierarchical Federated Edge Learning. *arXiv:2002.11343*.
- McMahan, B.; Moore, E.; Ramage, D.; Hampson, S.; and y Arcas, B. A. 2017a. Communication-efficient learning of deep networks from decentralized data. In *Artificial Intelligence and Statistics*, 1273–1282. PMLR.
- McMahan, H. B.; Moore, E.; Ramage, D.; Hampson, S.; et al. 2017b. Communication-efficient learning of deep networks from decentralized data. In *20th Int'l Conf. Artificial Intelligence and Statistics (AISTATS)*, 1273–1282.
- Nishio, T.; and Yonetani, R. 2019. Client selection for federated learning with heterogeneous resources in mobile edge. In *IEEE Int'l. Conf. on Communications*, 1–7.
- Parisi, G. I.; Kemker, R.; Part, J. L.; Kanan, C.; and Wermter, S. 2019. Continual lifelong learning with neural networks: A review. *Neural Networks* 113: 54–71.
- Sahu, A. K.; Li, T.; Sanjabi, M.; Zaheer, M.; Talwalkar, A.; and Smith, V. 2018. On the convergence of federated optimization in heterogeneous networks. *arXiv:1812.06127*.
- Sattler, F.; Müller, K.-R.; and Samek, W. 2020. Clustered federated learning: Model-agnostic distributed multitask optimization under privacy constraints. *IEEE Transactions on Neural Networks and Learning Systems*.
- Sattler, F.; Wiedemann, S.; Müller, K.-R.; and Samek, W. 2019. Robust and communication-efficient federated learning from non-iid data. *arXiv:1903.02891*.
- Shoham, N.; Avidor, T.; Keren, A.; Israel, N.; Benditkis, D.; Mor-Yosef, L.; and Zeitak, I. 2019. Overcoming Forgetting in Federated Learning on Non-IID Data. *arXiv:1910.07796*.
- Smith, V.; Chiang, C.-K.; Sanjabi, M.; and Talwalkar, A. S. 2017. Federated multi-task learning. In *Advances in Neural Information Processing Systems (NeurIPS)*, 4424–4434.

So, J.; Guler, B.; and Avestimehr, A. S. 2020. Turbo-Aggregate: Breaking the Quadratic Aggregation Barrier in Secure Federated Learning. *arXiv:2002.04156*.

Wang, J.; Sahu, A. K.; Yang, Z.; Joshi, G.; and Kar, S. 2019a. MATCHA: Speeding up decentralized SGD via matching decomposition sampling. *arXiv:1905.09435*.

Wang, S.; Tuor, T.; Salonidis, T.; Leung, K. K.; Makaya, C.; He, T.; and Chan, K. 2019b. Adaptive federated learning in resource constrained edge computing systems. *IEEE Journal on Selected Areas in Communications* 37(6): 1205–1221.

Xie, M.; Long, G.; Shen, T.; Zhou, T.; Wang, X.; and Jiang, J. 2020. Multi-Center Federated Learning. *arXiv:2005.01026*.

Yoon, J.; Jeong, W.; Lee, G.; Yang, E.; and Hwang, S. J. 2020. Federated Continual Learning with Weighted Inter-client Transfer. In *ICML 2020 Workshop in Lifelong Learning*.

Yoshida, N.; Nishio, T.; Morikura, M.; Yamamoto, K.; and Yonetani, R. 2019. Hybrid-FL: Cooperative learning mechanism using non-iid Data in wireless networks. *arXiv:1905.07210*.

Zhao, Y.; Li, M.; Lai, L.; Suda, N.; Civin, D.; and Chandra, V. 2018. Federated learning with non-iid data. *arXiv:1806.00582*.

Zhu, H.; and Jin, Y. 2019. Multi-objective evolutionary federated learning. *IEEE Trans. on Neural Networks and Learning Systems*.

A Convergence Analysis

In this section, we analyze convergence for *STAR-stars* and then extend it to the rest of architectures.

Convergence Analysis for *STAR-stars*

First of all, we make the following assumption for the loss function $F^{k,i}$, as in many other relevant studies (Liu et al. 2020; Wang et al. 2019b).

Assumption 1. For every i and k , (1) $F^{k,i}$ is convex; (2) $F^{k,i}$ is ρ -Lipschitz, i.e., $\|F^{k,i}(\mathbf{w}) - F^{k,i}(\mathbf{w}')\| \leq \rho\|\mathbf{w} - \mathbf{w}'\|$ for any \mathbf{w} and \mathbf{w}' ; and (3) $F^{k,i}$ is β -smooth, i.e., $\|\nabla F^{k,i}(\mathbf{w}) - \nabla F^{k,i}(\mathbf{w}')\| \leq \beta\|\mathbf{w} - \mathbf{w}'\|$ for any \mathbf{w} and \mathbf{w}' .

Under this assumption, Lemma 1 holds for the group and global loss functions. F_k , which is the loss function for a node group, is additionally considered here unlike Wang et al. (2019b).

Lemma 1. F and F^k are convex, ρ -Lipschitz, and β -smooth.

Proof. It is straightforward from Assumption 1 and the definitions of F and F^k in Definition 3. \square

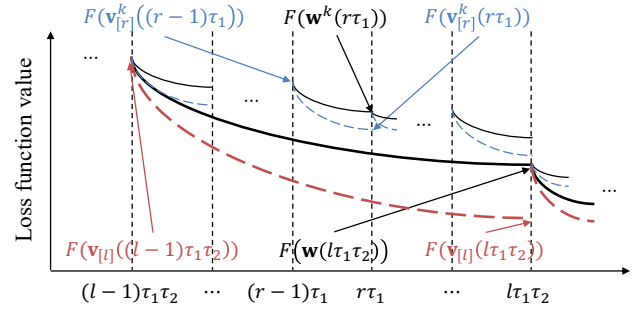


Figure 4: Illustration of loss divergence and synchronization between \mathbf{w}^k and $\mathbf{v}_{[r]}^k$ and between \mathbf{w} and $\mathbf{v}_{[l]}$.

We introduce two types of intervals depending on the learning level: a *group interval*, $[r] \triangleq [(r-1)\tau_1, r\tau_1]$, indicates an interval between two successive *group* aggregations, and a *global interval*, $[l] \triangleq [(l-1)\tau_1\tau_2, l\tau_1\tau_2]$, indicates an interval between two successive *global* aggregations.

Next, we introduce the notion of *group-based virtual learning* in Definition 9, where training data is assumed to exist on a *virtual* central repository for each model. This notion is used to bridge the *local-to-group divergence* (i.e., the divergence between a local model and a group model) in a group interval and the *group-to-global divergence* (i.e., the divergence between a group model and a global model) in a global interval.

Definition 9 (Group-Based Virtual Learning). Given a certain group membership \mathbf{z} , for any k , $[r]$, and $[l]$, the *virtual group model* $\mathbf{v}_{[r]}^k$ and *virtual global model* $\mathbf{v}_{[l]}$ are updated by performing gradient descent steps on the centralized data examples for \mathcal{N}^k and \mathcal{N} , respectively, and synchronized with the federated group model \mathbf{w}^k and the global model \mathbf{w} at the beginning of each interval, as in Eq. (5).

$$\begin{aligned} \mathbf{v}_{[r],t}^k &\triangleq \begin{cases} \mathbf{w}_t^k & \text{if } t = (r-1)\tau_1, \\ \mathbf{v}_{[r],t-1}^k - \eta\nabla F^k(\mathbf{v}_{[r],t-1}^k) & \text{otherwise} \end{cases} \\ \mathbf{v}_{[l],t} &\triangleq \begin{cases} \mathbf{w}_t & \text{if } t = (l-1)\tau_1\tau_2, \\ \mathbf{v}_{[l],t-1} - \eta\nabla F(\mathbf{v}_{[l],t-1}) & \text{otherwise} \end{cases} \end{aligned} \quad (5)$$

To facilitate the interpretation, Figure 4 shows how a virtual model \mathbf{v} is updated, following Definition 9. For example, $\mathbf{v}_{[l]}$ starts diverging from \mathbf{w} after $(l-1)\tau_1\tau_2$ and becomes synchronized with \mathbf{w} at $l\tau_1\tau_2$.

Then, we formalize *group-based gradient divergence* in Definition 10 that models the impact of the difference in data distributions across nodes on federated learning.

Definition 10 (Group-Based Gradient Divergence). Given a certain group membership \mathbf{z} , for any i and k , $\delta^{k,i}$ is defined as the gradient difference between the i -th local loss and the k -th group loss; Δ^k is defined as the gradient difference between the k -th group loss and the global loss, which can be

expressed as Eq. (6).

$$\begin{aligned}\delta^{k,i} &\triangleq \max_{\mathbf{w}} \|\nabla F^{k,i}(\mathbf{w}) - \nabla F^k(\mathbf{w})\|, \\ \Delta^k &\triangleq \max_{\mathbf{w}} \|\nabla F^k(\mathbf{w}) - \nabla F(\mathbf{w})\|\end{aligned}\quad (6)$$

Then, the *local-to-group divergence* δ and the *group-to-global divergence* Δ are formulated as Eq. (7).

$$\delta \triangleq \sum_{k \in \mathcal{G}} \sum_{i \in \mathcal{N}^k} \frac{|\mathcal{D}^{k,i}|}{|\mathcal{D}|} \delta^{k,i}, \quad \Delta \triangleq \sum_{k \in \mathcal{G}} \frac{|\mathcal{D}^k|}{|\mathcal{D}|} \Delta^k \quad (7)$$

Based on Definition 9 and 10, we introduce an auxiliary lemma (Lemma 2).

Lemma 2. For any $[r]$, $[l]$, and $t \in [(r-1)\tau_1, r\tau_1] \subset [(l-1)\tau_1\tau_2, l\tau_1\tau_2]$, an upper bound of the norm of the difference between a local model and the virtual global model can be expressed as Eq. (8).

$$\begin{aligned}\|\mathbf{w}_t^{k,i} - \mathbf{v}_{[l],t}\| &\leq \frac{\delta^{k,i}}{\beta} ((\eta\beta + 1)^{t-(r-1)\tau_1} - 1) \\ &\quad + \frac{\Delta^k}{\beta} ((\eta\beta + 1)^{t-(l-1)\tau_1\tau_2} - 1)\end{aligned}\quad (8)$$

Proof. From the triangle inequality, one can simply derive Eq. (9).

$$\begin{aligned}\|\mathbf{w}_t^{k,i} - \mathbf{v}_{[l],t}\| &= \|\mathbf{w}_t^{k,i} - \mathbf{v}_{[r],t}^k + \mathbf{v}_{[r],t}^k - \mathbf{v}_{[l],t}\| \\ &\leq \|\mathbf{w}_t^{k,i} - \mathbf{v}_{[r],t}^k\| + \|\mathbf{v}_{[r],t}^k - \mathbf{v}_{[l],t}\|\end{aligned}\quad (9)$$

To conclude this proof, it thus suffices to show Eq. (10) and (11).

$$\|\mathbf{w}_t^{k,i} - \mathbf{v}_{[r],t}^k\| \leq \frac{\delta^{k,i}}{\beta} ((\eta\beta + 1)^{t-(r-1)\tau_1} - 1) \quad (10)$$

$$\|\mathbf{v}_{[r],t}^k - \mathbf{v}_{[l],t}\| \leq \frac{\Delta^k}{\beta} ((\eta\beta + 1)^{t-(l-1)\tau_1\tau_2} - 1) \quad (11)$$

Then, by putting Eq. (10) and (11) into Eq. (9), we can confirm Lemma 2.

Both Eq. (10) and (11) can be easily drawn from the β -smooth property of $F^{k,i}$ and F^k . From Eq. (4) and (6), we can derive Eq. (12).

$$\begin{aligned}\|\mathbf{w}_t^{k,i} - \mathbf{v}_{[r],t}^k\| &= \|\mathbf{w}_{t-1}^{k,i} - \eta \nabla F^{k,i}(\mathbf{w}_{t-1}^{k,i}) - \mathbf{v}_{[r],t-1}^k + \eta \nabla F^k(\mathbf{v}_{[r],t-1}^k)\| \\ &\leq \|\mathbf{w}_{t-1}^{k,i} - \mathbf{v}_{[r],t-1}^k\| \\ &\quad + \eta \|\nabla F^{k,i}(\mathbf{w}_{t-1}^{k,i}) - \nabla F^{k,i}(\mathbf{v}_{[r],t-1}^k)\| \\ &\quad + \eta \|\nabla F^{k,i}(\mathbf{v}_{[r],t-1}^k) - \nabla F^k(\mathbf{v}_{[r],t-1}^k)\| \\ &\leq (\eta\beta + 1) \|\mathbf{w}_{t-1}^{k,i} - \mathbf{v}_{[r],t-1}^k\| + \eta \delta^{k,i}\end{aligned}\quad (12)$$

The last inequality stems from the β -smoothness of $F^{k,i}$ and Definition 10.

Then, since $\mathbf{w}_t^{k,i} = \mathbf{w}_t^k = \mathbf{v}_{[r],t}^k$ at every group aggregation from Eq. (4) and (6), Eq. (12) can be rewritten as

Eq. (13).

$$\begin{aligned}\|\mathbf{w}_t^{k,i} - \mathbf{v}_{[r],t}^k\| &\leq \eta \delta^{k,i} \sum_{y=1}^{t-(r-1)\tau_1} (\eta\beta + 1)^{y-1} \\ &= \frac{\delta^{k,i}}{\beta} ((\eta\beta + 1)^{t-(r-1)\tau_1} - 1)\end{aligned}\quad (13)$$

Analogously, one can derive Eq. (11). This is the end of the proof of Lemma 2. \square

From Lemma 2 and Jensen's inequality, for all t and q , we have Eq. (14).

$$\begin{aligned}\|\mathbf{w}_t - \mathbf{v}_{[l],t}\| &\leq \sum_{k \in \mathcal{G}} \sum_{i \in \mathcal{N}^k} \frac{|\mathcal{D}^{k,i}|}{|\mathcal{D}|} \|\mathbf{w}_t^{k,i} - \mathbf{v}_{[l],t}\| \\ &\leq \frac{\delta}{\beta} ((\eta\beta + 1)^{\tau_1} - 1) + \frac{\Delta}{\beta} ((\eta\beta + 1)^{\tau_1\tau_2} - 1)\end{aligned}\quad (14)$$

Finally, for *STAR-stars*, we derive the convergence bound between the federated global model and the virtual global model by Theorem 4.

Theorem 4 (Convergence Bound of *STAR-stars*). For any global interval $[l]$ and $t \in [l]$, if $F^{k,i}$ is β -smooth for every i and k in Eq. (6), then Eq. (15) holds.

$$\begin{aligned}F(\mathbf{w}_t) - F(\mathbf{v}_{[l],t}) &\leq \frac{\rho}{\beta} (\delta h(\tau_1) + \Delta h(\tau_1\tau_2)) \\ &\quad \text{where } h(t) \triangleq (\eta\beta + 1)^t - 1\end{aligned}\quad (15)$$

Convergence Analysis for the Other Architectures

In this section we analyze convergence bounds for flat architectures (*STAR* and *RING*), consensus group architectures (*STAR-rings*, *RING-stars*, and *RING-rings*, and pluralistic group architectures (*stars* and *rings*). First, the convergence bound of *STAR* is the same as that of *STAR-stars* with no group $|\mathcal{G}| = 1$ and no group communication $\tau_2 = 1$, as in Eq. (16). By excluding the notion of groups, it also means that the group-to-global divergence Δ becomes 0 and thus the local-to-group divergence δ becomes the local-to-global divergence D , which is extended from Eq. (6) and (7).

$$\begin{aligned}F(\mathbf{w}_t) - F(\mathbf{v}_{[l],t}) &\leq \frac{\rho}{\beta} Dh(\tau) \\ &\quad \text{where } D \triangleq \sum_{i \in \mathcal{N}} \frac{|\mathcal{D}^i|}{|\mathcal{D}|} D^i \\ &\quad \text{and } D^i \triangleq \max_{\mathbf{w}} \|\nabla F^i(\mathbf{w}) - \nabla F(\mathbf{w})\|\end{aligned}\quad (16)$$

Next, the convergence bound of *stars* is the same as multiple independent *STAR* groups, where the total node size of *stars* is the sum of nodes of each *STAR* group. Thus, by regarding the local-to-global divergence D from Eq. (16) of each *STAR* group as the local-to-group divergence δ^k of each group in *stars*, we have Eq. (17) for *stars*.

$$F(\mathbf{w}_t) - F(\mathbf{v}_{[l],t}) \leq \frac{\rho}{\beta} \delta h(\tau) \quad (17)$$

Next, for *STAR-rings*, similar to Theorem 1, each *ring*-based learning in a group is an unbiased estimator of the centralized learning within the group because of Eq. (18).

$$\mathbb{E}[\nabla F^{k,i}(\mathbf{w}_t)] = \sum_{i \in \mathcal{N}^k} \frac{|\mathcal{D}^{k,i}|}{|\mathcal{D}^k|} \nabla F^{k,i}(\mathbf{w}_t) = \nabla F^k(\mathbf{w}_t) \quad (18)$$

Then, by approximating $\nabla F^{k,i}(\mathbf{w}_t)$ of Eq. (6) to $\mathbb{E}[\nabla F^{k,i}(\mathbf{w}_t)]$ of Eq. (18), the local-to-group divergence δ becomes 0 and thus the group-to-global divergence Δ becomes the local-to-global divergence D . Thus, Eq. (15) is extended to Eq. (19) for *STAR-rings*.

$$F(\mathbf{w}_t) - F(\mathbf{v}_{[l],t}) \leq \frac{\rho}{\beta} Dh(\tau_1 \tau_2) \quad (19)$$

Next, for *RING-stars*, similar to Theorem 1, the global *RING*-based learning is an unbiased estimator of the globally centralized learning in consideration of each *stars*-based learning in a group because of Eq. (20).

$$\mathbb{E}[\nabla F^k(\mathbf{w}_t)] = \sum_{k \in \mathcal{G}} \frac{|\mathcal{D}^k|}{|\mathcal{D}|} \nabla F^k(\mathbf{w}_t) = \nabla F(\mathbf{w}_t) \quad (20)$$

Then, by approximating $\nabla F^k(\mathbf{w}_t)$ of Eq. (6) to $\mathbb{E}[\nabla F^k(\mathbf{w}_t)]$ of Eq. (20), the group-to-global divergence Δ becomes 0 and thus the local-to-group divergence δ becomes the local-to-global divergence D . Thus, Eq. (15) is extended to Eq. (21) for *RING-stars*.

$$F(\mathbf{w}_t) - F(\mathbf{v}_{[l],t}) \leq \frac{\rho}{\beta} Dh(\tau_1) \quad (21)$$

Analogously, from Theorem 1, *RING*, *Ring-rings*, and *rings* can be easily shown to have the approximate convergence bound of 0.

B Communication Scalability

In this section, we provide an approach to measure communication scalability. For the analysis, M denotes the model size; and given the total learning steps T , $\tau_f \triangleq T/\tau$ is defined as the number of global communications for the flat architectures; $\tau_c \triangleq T/\tau_1 \tau_2$ is defined as the number of global communications for the consensus group architectures; $\tau_p \triangleq T/\tau$ is defined as the number of group communications for the pluralistic group architectures.

STAR sends $M|\mathcal{N}|\tau_f$ of total global aggregation data; *RING* sends $M\tau_f$ of total global inter-node transfer because only one node is active for the diurnal property; *STAR-stars* sends $M|\mathcal{N}|(\tau_2 - 1)\tau_c$ of total group aggregation data and $M|\mathcal{N}|\tau_c$ of total global aggregation data, thus $M|\mathcal{N}|\tau_2 \tau_c$ of total communication data, which is the same cost as *STAR* in case of $\tau_f = \tau_2 \tau_c$ as suggested by Liu et al. (2020); *stars* sends $M|\mathcal{N}|\tau_p$ of total group aggregation data, which is the same cost as *STAR* because $\tau_p = \tau_f$ from the definition; analogously, one can show the total communication data size for the rest of architectures, as summarized in Table 1.

C Deferred Proofs

Theorem 1. *RING* is an unbiased estimator of the centralized learning that learns a centralized model by assuming the federated datasets to be located at a centralized storage.

Proof. The centralized learning is defined as Eq. (22).

$$\mathbf{w}_t = \mathbf{w}_{t-1} - \eta \nabla F(\mathbf{w}_{t-1}) \quad (22)$$

Next, for *RING* update, we regard the model and data communication relationship as the opposite, that is, instead of *RING* transferring a local model from one node to another while data stays in place, *RING* is redefined as switching data from one node to another while the local model stays in a certain node. Thus, at the time t of data transfer from node i to the certain node, Eq. (3) changes to Eq. (23). Note that the index for the certain node is not denoted because it does not need be distinguished from the others.

$$\mathbf{w}_t = \mathbf{w}_{t-1} - \eta \nabla F^i(\mathbf{w}_{t-1}) \quad (23)$$

Thus, Eq. (23) equals the centralized learning in expectation because of Eq. (24)

$$\mathbb{E}[\nabla F^i(\mathbf{w}_{t-1})] = \sum_{i \in \mathcal{N}} \frac{|\mathcal{D}^i|}{|\mathcal{D}|} \nabla F^i(\mathbf{w}_{t-1}) = \nabla F(\mathbf{w}_{t-1}) \quad (24)$$

□

Theorem 2. The convergence bound $O(\delta h(\tau))$ of *stars* doesn't necessarily be better than $O(Dh(\tau))$ of *STAR*.

Proof. From Eq. (6) and triangle inequality, we have Eq. (25).

$$\begin{aligned} \delta^{k,i} &= \max_{\mathbf{w}} \|\nabla F^{k,i}(\mathbf{w}) - \nabla F^k(\mathbf{w})\| \\ &= \max_{\mathbf{w}} \|\nabla F^{k,i}(\mathbf{w}) - \nabla F(\mathbf{w}) + \nabla F(\mathbf{w}) - \nabla F^k(\mathbf{w})\| \\ &\leq \max_{\mathbf{w}} [\|\nabla F^{k,i}(\mathbf{w}) - \nabla F(\mathbf{w})\| + \|\nabla F(\mathbf{w}) - \nabla F^k(\mathbf{w})\|] \end{aligned} \quad (25)$$

By summing Eq. (25) for all i and k and considering Eq. (7) and (16), we have Eq. (26).

$$\delta \leq \Delta + D \quad (26)$$

Similarly, from Eq. (16) and triangle inequality, we have Eq. (27).

$$\begin{aligned} D^i &= \max_{\mathbf{w}} \|\nabla F^i(\mathbf{w}) - \nabla F(\mathbf{w})\| \\ &= \max_{\mathbf{w}} \|\nabla F^i(\mathbf{w}) - \nabla F^k(\mathbf{w}) + \nabla F^k(\mathbf{w}) - \nabla F(\mathbf{w})\| \\ &\leq \max_{\mathbf{w}} [\|\nabla F^i(\mathbf{w}) - \nabla F^k(\mathbf{w})\| + \|\nabla F^k(\mathbf{w}) - \nabla F(\mathbf{w})\|] \end{aligned} \quad (27)$$

By summing Eq. (27) for all i and considering Eq. (7), we have Eq. (28).

$$D \leq \delta + \Delta \quad (28)$$

Lastly, based on Eq. (26) and (28), we can infer that the worst case of δ equals $\Delta + D$ that is larger than D , in which *STAR* achieves lower convergence bound than *stars*. □

Theorem 3. *RING* exhibits higher variance than the centralized learning (unbiased estimator of *RING* from Theorem 1).

Algorithm 2: Tornadoes (STAR-rings)

INPUT : $\mathcal{N}, |\mathcal{G}|, C, \tau_1, \tau_2$
OUTPUT: \mathbf{w}_T

- 1 Initialize $\{\mathbf{w}_0^{k,i}\}_{i \in \mathcal{N}}$ to a random model \mathbf{w}_0
- 2 Initialize a random ring $[i_j \in \mathcal{N} | j \in \mathbb{N}^0, i_{j+|\mathcal{N}|} = i_j]$
- 3 $\{\mathcal{N}^k\}_{k \in \mathcal{G}} \leftarrow \text{CLUSTER}(\mathcal{N})$ // Algorithm 3
- 4 **for** $t \leftarrow 0, \dots, T-1$ **do**
- 5 **for each** $k \in \mathcal{G}$ **in parallel do**
- 6 **for each** $c \leftarrow 0, \dots, C-1$ **in parallel do**
- 7 $j \leftarrow \lfloor t/\tau_1 \rfloor, i \leftarrow (i_j + c) \bmod |\mathcal{N}^k|$
- 8 $\mathbf{w}_{t+1}^{k,i} \leftarrow \mathbf{w}_t^{k,i} - \eta \nabla F^{k,i}(\mathbf{w}_t^{k,i})$
- 9 **if** $t \bmod \tau_1$ **and** $t \bmod \tau_1 \tau_2 \neq 0$ **then**
- 10 $i_{next} \leftarrow (i_{j+1} + c) \bmod |\mathcal{N}^k|$
- 11 $\mathbf{w}_t^{k,i_{next}} \leftarrow \mathbf{w}_t^{k,i}$
- 12 **if** $t \bmod \tau_1 \tau_2 = 0$ **then**
- 13 $\{\mathbf{w}_t^{k,i}\}_{k \in \mathcal{G}, i \in \mathcal{N}} \leftarrow \sum_{k \in \mathcal{G}} \sum_{i \in \mathcal{N}^k} \frac{|\mathcal{D}^{k,i}|}{|\mathcal{D}|} \mathbf{w}_t^{k,i}$

Proof. First, from the β -smoothness of F and Eq. (22), we have Eq. (29) for centralized learning.

$$\begin{aligned} F(\mathbf{w}_t) &= F(\mathbf{w}_{t-1} - \eta \nabla F(\mathbf{w}_{t-1})) \\ &\leq F(\mathbf{w}_{t-1}) - \eta(1 - \frac{\eta\beta}{2}) \|\nabla F(\mathbf{w}_{t-1})\|^2 \end{aligned} \quad (29)$$

Next, from the β -smoothness of F and the definition of *RING* update in Eq. (23), we have Eq. (30) for *RING*.

$$\begin{aligned} F(\mathbf{w}_t) &= F(\mathbf{w}_{t-1} - \eta \nabla F^i(\mathbf{w}_{t-1})) \\ &\leq F(\mathbf{w}_{t-1}) + \nabla F(\mathbf{w}_{t-1})(-\eta \nabla F^i(\mathbf{w}_{t-1})) \\ &\quad + \frac{\eta^2 \beta}{2} \|\nabla F^i(\mathbf{w}_{t-1})\|^2 \end{aligned} \quad (30)$$

In expectation with regard to i , we have Eq. (31).

$$\begin{aligned} F(\mathbf{w}_t) &\leq F(\mathbf{w}_{t-1}) - \eta \|\nabla F(\mathbf{w}_{t-1})\|^2 \\ &\quad + \frac{\eta^2 \beta}{2} \mathbb{E}_i \|\nabla F^i(\mathbf{w}_{t-1})\|^2 \\ &\leq F(\mathbf{w}_{t-1}) - \eta(1 - \frac{\eta\beta}{2}) \|\nabla F(\mathbf{w}_{t-1})\|^2 \\ &\quad + \frac{\eta^2 \beta}{2} [\mathbb{E}_i \|\nabla F^i(\mathbf{w}_{t-1})\|^2 - \|\mathbb{E}_i \nabla F^i(\mathbf{w}_{t-1})\|^2] \end{aligned} \quad (31)$$

where $\mathbb{E}_i \|\nabla F^i(\mathbf{w}_{t-1})\|^2 - \|\mathbb{E}_i \nabla F^i(\mathbf{w}_{t-1})\|^2$ is the learning variance of *RING*, which is an added term from Eq. (29).

Analogously, one can show similar variances for *STAR-rings*, *RING-stars*, *Ring-rings*, and *rings*. \square

D TornadoAggregate Details

Algorithm 2 shows the overall procedure of Tornadoes that takes the node set \mathcal{N} and the number of groups $|\mathcal{G}|$, chains C , epochs τ_1 , and communication rounds τ_2 as input and returns the final model \mathbf{w}_T as output. It begins by initializing all local models $\mathbf{w}_0^{k,i}$, a randomly permuted inter-node ring

Algorithm 3: Grouping Scheme

- 1 **function** GROUP_BY_IID(\mathcal{N}):
- 2 $\text{COST}_A(i, k) \triangleq \text{EMD}(\mathcal{D}^k, \mathcal{D})$
- 3 $\text{COST}_U(i, k) \triangleq \text{EMD}(\mathcal{D}^{k,i}, \mathcal{D})$
- 4 **return** GROUP($\mathcal{N}, \text{COST}_A, \text{COST}_U$)
- 5
- 6 **function** CLUSTER(\mathcal{N}):
- 7 $\text{COST}_A(i, k) \triangleq \text{EMD}(\mathcal{D}^{k,i}, \mathcal{D}^k)$
- 8 $\text{COST}_U(i, k) \triangleq \text{EMD}(\mathcal{D}^{k,i}, \mathcal{D}^k)$
- 9 **return** GROUP($\mathcal{N}, \text{COST}_A, \text{COST}_U$)
- 10
- 11 **function** GROUP($\mathcal{N}, \text{COST}_A, \text{COST}_U$):
- 12 Select random medoid nodes \mathcal{N}_m of size $|\mathcal{G}|$
- 13 $\mathbf{z} \leftarrow [\arg \min_{k \in \mathcal{G}} \text{COST}_A(i, k) | \forall i \in \mathcal{N}]$
- 14 **while** the last COST_A is not steady **do**
- 15 $\mathcal{N}_m \leftarrow [\arg \min_{i \in \mathcal{N}^k} \text{COST}_U(i, k) | \forall k \in \mathcal{G}]$
- 16 $\mathbf{z} \leftarrow [\arg \min_{k \in \mathcal{G}} \text{COST}_A(i, k) | \forall i \in \mathcal{N}]$
- 17 **return** $\{\{i | (i, k) \in \mathbf{z}, k = k'\} | k' \in \mathcal{G}\}$

$[i_j]$, and group indices $\{\mathcal{N}^k\}$ by clustering nodes (Lines 1–3). Then, for each group and each chain of the group, the local updates are performed at the node i (Lines 5–8); every τ_1 epochs, each local model is transferred to the next node i_{next} within the same group k (Lines 9–11); every $\tau_1 \tau_2$ steps, the global model is learned by aggregating all local models and then broadcasts back to all nodes (Lines 12–13). Overall, Lines 4–13 repeat for T steps.

We derive another heuristic of TornadoAggregate with *rings* architecture, called Tornado-rings, which is the same as Tornadoes without the global aggregation to develop an independent and specialized model for each group, i.e., Lines 12–13 of Algorithm 2 are not executed for Tornado-rings. We note that, for the *stars* and *rings*, the test performance are measured with the group model of each independent group.

Algorithm 3 shows the *two* grouping schemes: GROUP_BY_IID and CLUSTER. Both functions define their own association cost COST_A and update cost COST_U and, in turn, call GROUP function with the defined costs. The costs are based on the EMD (earth mover distance) that can approximately model the learning divergences, as proposed by Zhao et al. (2018), which can be expressed as Eq. (32). In GROUP_BY_IID function (Lines 1–4), a group data distribution $\mathcal{D}^{k,i}$ is compared with the global dataset \mathcal{D} to improve the group-to-global divergence Δ of Eq. (6), while in CLUSTER function (Lines 6–9), a local data distribution $\mathcal{D}^{k,i}$ is compared with a group data distribution \mathcal{D}^k to improve the local-to-group divergence δ of Eq. (6). It should be noted that for the COST_U of GROUP_BY_IID function, we had no choice but to use $\mathcal{D}^{k,i}$ instead of \mathcal{D}^k because a cost related to a node should be returned to determine a new medoid node.

$$\begin{aligned} \text{EMD}(\mathcal{D}_1, \mathcal{D}_2) &\triangleq \sum_{\forall class} |\mathbb{P}(y_j = class | j \in \mathcal{D}_1) - \mathbb{P}(y_j = class | j \in \mathcal{D}_2)| \end{aligned} \quad (32)$$

Dataset	Initial Cost	Final Cost
FedShakespeare	0.391	0.375 (4.3% reduced)
MNIST	0.728	0.474 (53.6% reduced)

Table 3: **Reduction of clustering cost in Algorithm 3.**

The GROUP function aims at finding subsets of node indexes for all groups $\{\mathcal{N}^k\}_{k=1\dots|\mathcal{G}|}$ such that it reduces the defined costs to the extent possible. For this purpose, it begins by selecting random medoid nodes \mathcal{N}_m of size $|\mathcal{G}|$ (Line 12). Then, it iteratively updates \mathbf{z} by minimizing COST_A for all nodes and COST_U for all groups until the cost is steady (Lines 14–16).

E Supplementary Evaluation

Experimental Setting

Configuration We used FedML (He et al. 2020), one of the most widely used simulation frameworks for federated learning, on PyTorch 1.6.0 to extensively evaluate the performance of various datasets, models, and algorithms.

Parameters The parameters for both FedShakespeare on RNN and MNIST on logistic regression benchmarks followed those suggested by FedML. The benchmarks used SGD (Stochastic Gradient Descent) optimizer with the learning rate of 0.03. In addition, we randomly sampled 100 nodes for both train and test phase, out of 715 nodes for FedShakespeare and 1000 nodes for MNIST.

Table 4 shows the parameters used for each algorithm. In particular, for the group size, we applied the aforementioned *small ring* principle to all algorithms such that the group size of an algorithm with IID node grouping, random grouping, and node clustering is set to 2, 5, and 10, respectively, where 10 is considered a reasonably large value for the group size; for the number of chains, we applied the *ring chaining* principle to the proposed TornadoAggregate heuristics such that the number of chains is set to the number of groups, which is the maximum value by definition; for the communication interval, we firstly determined the product of τ_1 and τ_2 of HierFAVG to be equal to τ of FedAVG so that HierFAVG can improve accuracy by sacrificing little communication cost, as suggested by Liu et al. (2020), and then we set the same parameters as HierFAVG for the rest of algorithms.

Additional Results

Figure 5 shows the train loss and accuracy of *nine* algorithms on FedShakespeare dataset. Even though HierFAVG seemingly outrun the others, compared with the test accuracy of HierFAVG in Figure 2, we can infer that it overfit towards the training dataset. Similar to the aforementioned results of IFCA, Tornado-rings performed bad because of the small reduction of clustering cost, defined in Algorithm 3, for FedShakespeare dataset, as shown in Table 3. Low accuracy of SemiCyclic algorithm can be attributed to the low data

utilization with low number of active nodes, which is also pointed out by Ding et al. (2020).

Figure 6 shows the train loss and accuracy of all algorithms on MNIST dataset. Interestingly, in contrast to the results for FedShakespeare dataset, Tornado-rings significantly outperformed the others except for closely following IFCA. The reason why the worst performers became the best performers can also be attributed to the large reduction clustering cost, as shown in Table 3. To strike the balance between the two extremes, we leave Tornado-rings as our future work. Aside from Tornado-rings and IFCA, Tornadoes outperformed the others and the rest of algorithms exhibited the similar performance trend to that from FedShakespeare.

F Future Directions

We consider the following works orthogonal to our work, which can thus be easily extended to by TornadoAggregate.

- **Communication Reduction Techniques:** This category includes quantization (Konečný et al. 2016a,b), compression (Sattler et al. 2019), or dropout (Caldas et al. 2018).
 - **Communication-Aware Learning:** This category includes adaptive communication interval (Wang et al. 2019b), communication-constrained learning (Nishio and Yonetani 2019; Yoshida et al. 2019), or multi-objective optimization of learning error and communication (Zhu and Jin 2019).
 - **Global-Information Sharing:** This category includes sharing a subset of global IID data samples (Zhao et al. 2018; Yoshida et al. 2019), sharing a subset of global data features to scale up the feature-related parameters of a local optimizer (Konečný et al. 2016a), or sharing a generative model that can produce an augmented IID dataset (Smith et al. 2017; Jeong et al. 2018).
- On the other hand, we aim at improving TornadoAggregate in the following directions.
- **Client Sampling:** Client sampling techniques (McMahan et al. 2017b; Sahu et al. 2018; Li et al. 2020) introduce a different variance aspect from those handled in this study.
 - **Peer-to-Peer Learning:** Other than the star and ring architectures, peer-to-peer (P2P) federated learning (Wang et al. 2019a; Hegedűs, Danner, and Jelasity 2019; Wang et al. 2019a) should also be considered.
 - **Transfer Learning:** In all synchronizations, model parameters are set to the previously learned model parameters, but we can also consider transferring parameters between different types of models (Jeong et al. 2018; Li and Wang 2019; He, Avestimehr, and Annavaram 2020).
 - **Continual Learning:** We can extend TornadoAggregate to the novel techniques in the field of continual learning, such as weight decomposition (Yoon et al. 2020) or loss regularization (Shoham et al. 2019).
 - **Algorithm Optimization:** Other than EMD of Eq. (32), IIDness can also be quantified by loss divergence (Li et al. 2020), gradient divergence (Wang et al. 2019b), or weight divergence (Zhao et al. 2018).

Hierarchy	Algorithm	Architecture	Grouping Scheme	Group Size	# Chain	Communication Interval
Flat	FedAvg (McMahan et al. 2017b)	<i>STAR</i>	-	1	-	$\tau = 100$
Consensus Group	HierFAVG (Liu et al. 2020)	<i>STAR-stars</i>	Random	5	-	$\tau_1 = 10, \tau_2 = 10$
	Astraea (Duan et al. 2020)	<i>STAR-rings</i>	IID	2	1	$\tau_1 = 10, \tau_2 = 10$
	MM-PSGD (Ding et al. 2020)	<i>RING-stars</i>	Cluster	10	1	$\tau_1 = 10, \tau_2 = 10$
	Tornado (Proposed)	<i>RING-stars</i>	IID	2	2	$\tau_1 = 10, \tau_2 = 10$
	Tornadoes (Proposed)	<i>STAR-rings</i>	Cluster	10	10	$\tau_1 = 10, \tau_2 = 10$
Pluralistic Group	IFCA (Ghosh et al. 2020))	<i>stars</i>	Cluster	10	-	$\tau = 100$
	SemiCyclic (Eichner et al. 2019)	<i>rings</i>	Random	5	1	$\tau = 100$
	Tornado-rings (Proposed)	<i>rings</i>	Cluster	10	10	$\tau = 100$

Table 4: Algorithm parameters.

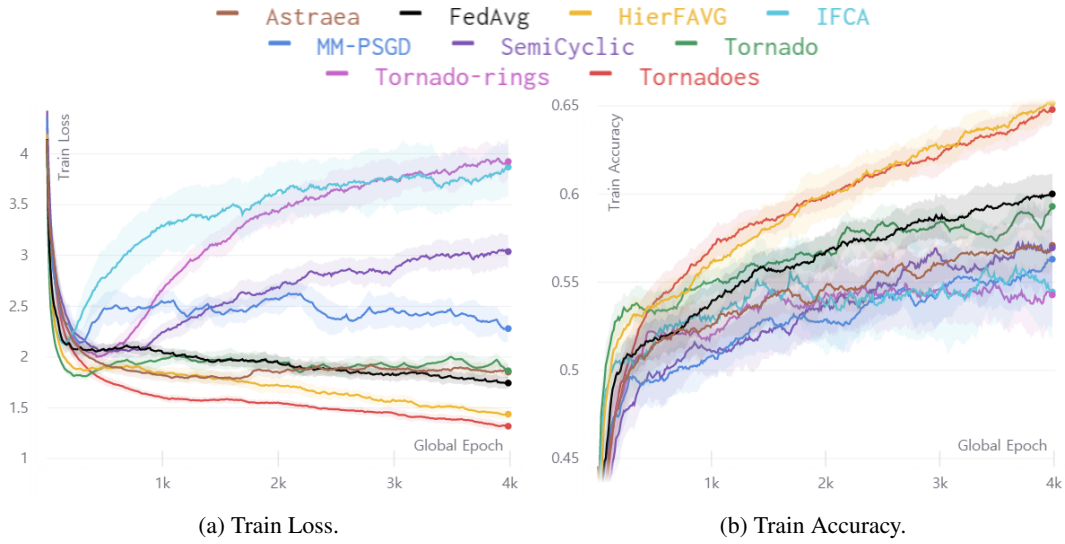


Figure 5: FedShakespeare.

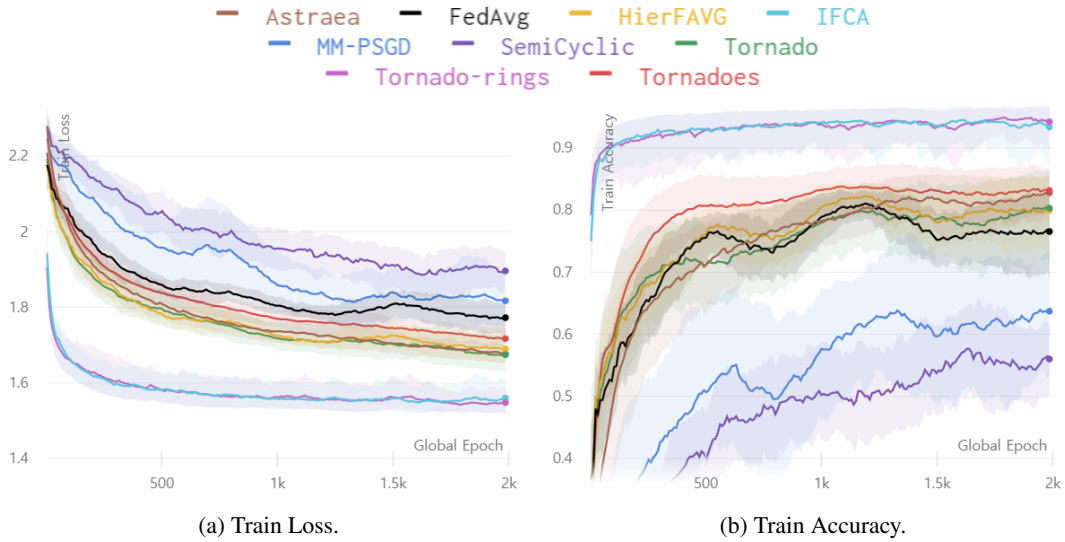


Figure 6: MNIST.